Stress evolution during ripening of self-assembled InAs/GaAs quantum dots

D. M. Schaadt,[a] D. Z. Hu, and K. H. Ploog
Paul-Drude-Institut für Festkörperelektronik, Hausvogteiplatz 5-7, D-10117 Berlin, Germany

(Received 15 January 2006; accepted 5 March 2006; published 25 July 2006)

We have investigated the annealing behavior of InAs quantum dots (QDs) grown on GaAs(001) substrates by molecular beam epitaxy. An *in situ* cantilever beam setup was employed to record the stress evolution during deposition and subsequent annealing at the growth temperature. *Ex situ* atomic force microscopy (AFM) was used to characterize the morphological evolution of the QDs. During growth of InAs QDs, a stress of 4.05 ± 0.5 GPa develops in the wetting layer. Beyond a critical thickness of 1.5–1.6 monolayer, the strain is relieved by the QD formation. During subsequent annealing the build-up stress relaxes. For annealing at temperatures around 440 and 470 °C, QDs undergo standard ripening. Models based on different mechanisms for Ostwald ripening, namely, kinetic and diffusion limited, are developed and fitted to the stress relaxation curves. Although the relaxation curve for annealing at 440 °C can be fitted reasonably well with all models, the model describing ripening limited by diffusion along dot boundaries yields a slightly better fit. On the other hand, at 455 and 470 °C, the relaxation curve can be fitted very well only with the model in which ripening is controlled by attachment/detachment of atoms on the dot surface. For samples grown and annealed at 500 °C, the stress accumulated during QD formation relaxes below the value which was built up by wetting-layer growth. AFM images taken at different annealing stages reveal that the QDs ripen first and then dissolve after 7.5–10 min annealing. These observations are explained by a combination of In desorption and interdiffusion between Ga and In. © *2006 American Vacuum Society.* [DOI: 10.1116/1.2218869]

I. INTRODUCTION

Self-organized quantum dots (QDs) have been extensively studied in recent years because of their potential for technological applications.[1] In heteroepitaxial systems with lattice mismatch ⩾2%, such as Si/Ge (4.1%) and InAs/GaAs (7.2%), quantum dots grow in the Stranski-Krastanow mode.[2] Typically, a transition to three-dimensional (3D) dot growth occurs after deposition of a two-dimensional (2D) wetting layer (WL) due to the mismatch stress between substrate and film. This misfit stress relaxes during and after dot formation.[3] For InAs/GaAs(001), the transition from 2D layer by layer growth to 3D QD growth is found to depend on the growth temperature and is at a thickness of 1.5–1.7 ML (monolayer).[4] If the amount of deposited material is small, the 3D dots are dislocation-free (so called coherent). Upon postgrowth annealing, these coherent islands undergo morphological changes with time, known as Ostwald ripening.[5] In the case of InAs/GaAs, ripening from many small to few large dots has been reported.[6,7]

The fundamental theory of particle coarsening is already well established by Lifshitz and Slezov[8] and Wagner[9] and further developed by Vengrenovitch[10] and Vengrenovitch *et al.*[11] where a dot size distribution and a mean dot size as a function of time are derived. The major assumption is that the total volume of the quantum dots remains constant, i.e., that there is no mass transfer between the QDs and the WL or substrate and that no desorption of material occurs. Therefore these theories should only be applied to ripening at low temperatures. Typically, the coarsening of particles is limited by various possible mechanisms. For ripening of InAs QDs, the following three models have to be considered. The first model, denoted as model 1, describes that coarsening is limited by a kinetic process. In the second and third models, denoted as models 2 and 3, respectively, ripening is controlled by diffusion on the surface (model 2) and along the dot boundaries (model 3). To determine the ripening process of QDs, investigators often try to fit an experimentally obtained mean island radius to the above mentioned theoretical models. However, this procedure does not always yield a clear determination of the ripening process. For instance, for annealing of InAs QDs, Krzyzewski and Jones[7] using scanning tunneling microscopy (STM) images taken at different annealing times found that the evolution of the average dot size as a function of time cannot be described by any of the above models. A better approach is to determine the ripening process by not fitting only the average dot radius but rather by fitting the complete time evolution of the dot radius distribution function to experimental data. For this purpose, we use an *in situ* cantilever beam setup to measure the film force evolution during deposition and annealing of InAs QDs grown on GaAs(001). The stress is then given by the slope in the film force curves. We can fit the models to film force relaxation curves obtained during the annealing phase. In combination with atomic force microscopy (AFM) images taken at various times during annealing, we are able to determine the involved ripening mechanism. For InAs/GaAs annealed at high temperatures, the above models should not

[a]Electronic mail: dschaadt@pdi-berlin.de

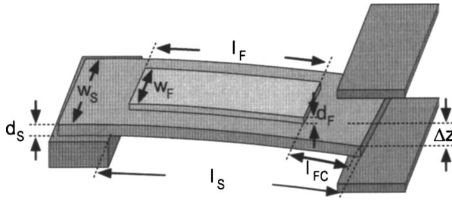

FIG. 1. Schematic drawing of the cantilever beam setup. The short side of the substrate stripe is along the $\langle 01\bar{1}\rangle$ direction, while the long side is along the $\langle 011\rangle$ direction.

be applied due to nonconstant nature of the total dot volume. For instance, dissolution of QDs occurs as Heyn[12] and Lee *et al.*[13] observed in the transition in reflection high energy electron diffraction (RHEED) patterns. They attributed the dissolution of InAs QDs to the desorption of In. However, it has also been reported[14] that intermixing of GaAs with InAs is significant at higher temperatures and it was observed that the mean dot volume increases due to the additionally incorporated GaAs.[15] Further, it was found that interdiffusion has a pronounced effect on the dissolution of embedded InAs QDs in GaAs,[16] but no report has been published that investigates the influence of interdiffusion on the ripening of uncapped QDs. We therefore also study the effect of annealing at higher temperatures. Our experimental results reveal that although In desorption influences the ripening behavior of QDs seriously, the dissolution of QDs is a result of combined In desorption and interdiffusion between Ga and In.

II. EXPERIMENTAL PROCEDURE

The samples were prepared in a III-V semiconductor molecular beam epitaxy chamber equipped with a cantilever beam setup to measure stress curves during growth and annealing. The epiready GaAs(001) substrate stripes measuring $25\times 5\times 0.15\ \mathrm{mm}^3$ were clamped on one side, while the other side was placed between two capacitor plates and allowed to bend freely, as shown in Fig. 1. A capacitance technique combined with a lock-in assisted signal detection system was used to measure a signal S_{meas} corresponding to the deflection Δz of the free end in real time.[17] The setup was calibrated by measuring a signal S_{cal} obtained from the bending of the cantilever due to its own weight. Applying Stoney's equation,[18] the film force F_F, defined as the force per film width w_F, is then given by

$$F_F=\frac{\rho_S g l_S^4\left(1-(4/3)\dfrac{l_{\mathrm{cal}}}{l_S}\right)}{2(1-\nu_S)l_F(l_F+2l_{FC})}\frac{w_S^2}{w_F}\frac{S_{\mathrm{meas}}}{S_{\mathrm{cal}}}, \tag{1}$$

where w_S is the substrate width, l_S is the substrate length, l_{cal} is half the length of the substrate inside the capacitor plates, ρ_S is the density of the substrate, l_{FC} is the gap between film end and substrate end, ν_S is the Poisson ratio of the substrate, and l_F is the film length. Before InAs deposition, the GaAs substrates were degassed at 300 °C (thermocouple reading) for 2 h followed by oxide desorption at 605 °C. Then, a 500 nm thick GaAs buffer layer was deposited. From previous studies,[3] it is known that the critical thickness for dot formation is around 1.5–1.6 ML in the temperature range of 440 and 500 °C used in this study. For comparison, films only consisting of a wetting layer were grown by depositing ~1.5 ML InAs, while films consisting of a wetting layer and quantum dots were grown by depositing nominally ~2.3 ML InAs, respectively. To investigate the ripening of QDs, these films remained uncapped. The annealing behavior of the quantum dots was monitored by keeping the samples at the growth temperature up to 10 min while recording the film force and then rapidly quenching them to room temperature for AFM studies. High-resolution transmission electron microscopy (HRTEM) was used to determine the structural properties.[19,20]

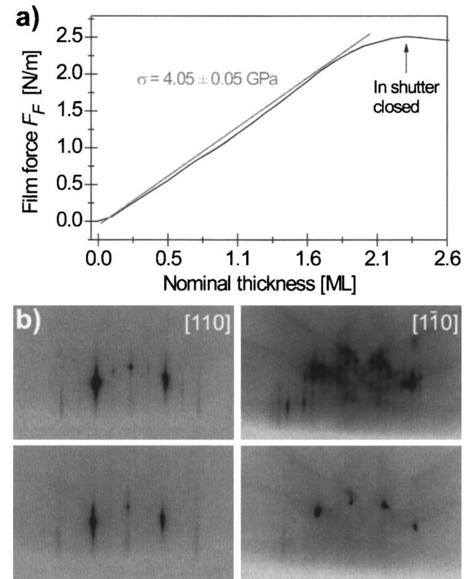

FIG. 2. (a) Film force measured during deposition of nominally 2.3 ML InAs at 440 °C. A linear increase (gray line) in film force is observed up to a critical thickness of about 1.6 ML, yielding a stress of about 4.6 GPa. (b) RHEED images taken in two azimuths before growth (top row) and deposition of 2.1 ML InAs (bottom row), showing the onset of a transition from 2D diffraction streaks to 3D Bragg spots.

III. RESULTS

A. Growth

Figure 2(a) displays the film force measured during growth of a nominally 2.3 ML thick InAs film at 440 °C. Upon opening of the In shutter, a linear increase in film force to ~1.8–1.95 N/m is observed up to a thickness of ~1.5–1.6 ML. With further InAs deposition, the film force increase becomes smaller and proceeds with decreasing slope up to a value of 2.5 N/m. AFM images reveal that no InAs dots are formed at thicknesses below 1.5 ML, thus suggesting that the thickness at which the slope starts decreasing corresponds to the critical thickness θ_c at which the QDs nucleate. This is consistent with the observation of a transition from 2D diffraction streaks to 3D spots in RHEED patterns [shown in Fig. 2(b)] obtained during growth. The observed θ_c=1.5–1.6 ML is also in good agreement with the

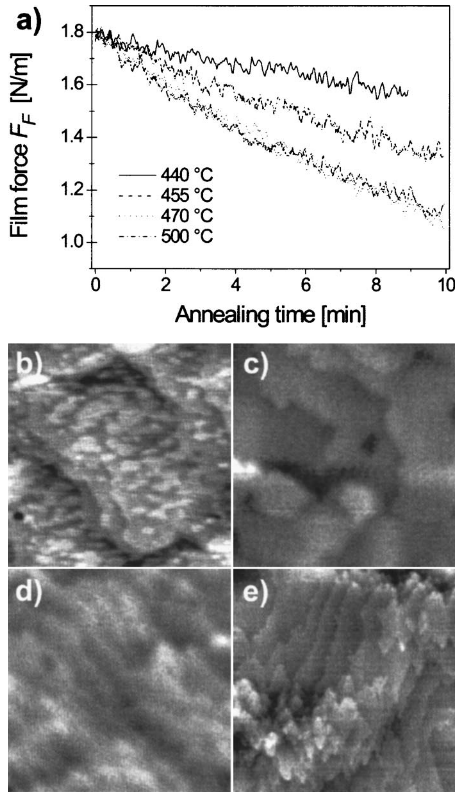

FIG. 3. (a) Film force curves obtained during annealing of 1.5 ML thick InAs films, i.e., samples consisting of the wetting layer only. A decrease in film force during annealing is visible; this effect becomes more pronounced with increasing annealing temperature. (b) 2×2 μm^2 AFM images of the WL samples taken (b) before annealing and after annealing for 10 min at (c) 440 °C, (d) 470 °C, and (e) 500 °C, respectively. The z scale is 1 nm for both images.

values reported in the literature for QD growth at 470 °C (e.g., Ref. 4). Quantitatively, our experiments yield a stress of about 4.05 ± 0.05 GPa, which is in reasonable agreement with the theoretical value of 5.3 GPa, given the measurement errors in both film force and growth rate. This indicates that the elastic properties of a monolayer of InAs are similar to those of InAs bulk crystals and that the influence of surface stress effects is negligible.[3]

B. Annealing

1. Wetting layer

Figure 3(a) shows the film force curves measured during annealing of 1.5 ML thick InAs film, i.e., film composed of the wetting layer only. We observe a decrease of the film force from 1.8 to 1.6, 1.35, 1.1, and 1.0 N/m for annealing at 440, 455, 470, and 500 °C, respectively. This decrease corresponds to a release of the mistfit stress accumulated during growth. The small decrease of film force for annealing at low temperatures indicates that the pseudomorphic wetting layer does not change during annealing. This is confirmed by an AFM taken after annealing for 10 min at 440 °C [Fig. 3(b)], which shows large terraces on the surface and an identical morphology to AFM images recorded before annealing (not shown). On the other hand, the higher the annealing temperature, the larger the decrease in film force. Corresponding AFM images taken after 10 min of annealing show that the surface contains more steps the higher the annealing temperature, which might be attributed to a mechanism for stress release.

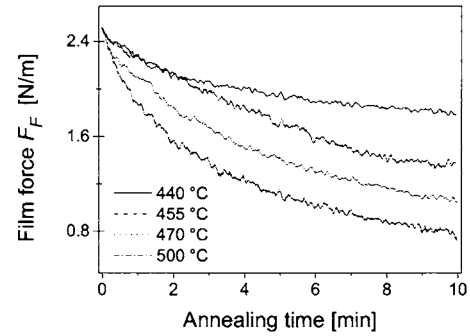

FIG. 4. Film force curves obtained during annealing of nominally ~2.1 ML thick InAs films, i.e., samples consisting of the uncapped quantum dots on top of wetting layer. The film force decreases more with increasing annealing temperature.

2. Quantum dots

During annealing of the quantum dot films, the film force also decreases with increasing annealing time, as shown in Fig. 4. Again, the effect becomes larger with increasing annealing temperature. For 440 °C, the film force decreases from about 2.5 to about 1.8 N/m, thereby approaching the value reached during the deposition of the wetting layer. Since the wetting layer changes only slightly during annealing at 440 °C, the decrease in F_F measured for the quantum dot film indicates a rearrangement of the dots yielding a reduction of the film stress. This effect can be clearly seen in AFM images taken at various stages during annealing, as shown in Fig. 5 (top row). The dots display standard Ostwald ripening from many small to few large dots, thereby reducing

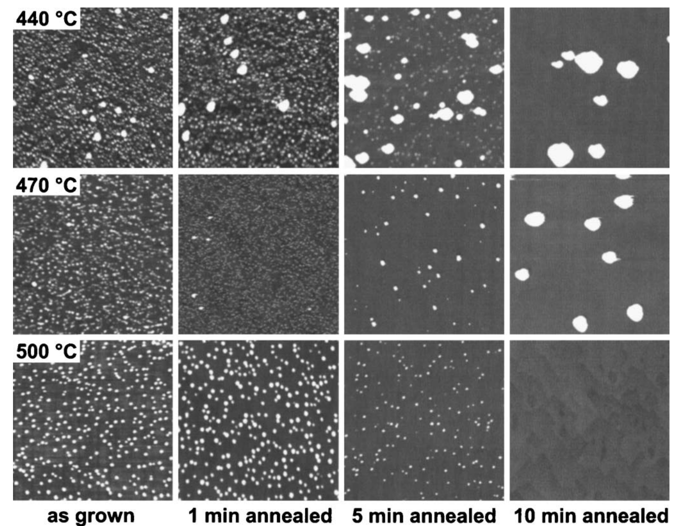

FIG. 5. 2×2 μm^2 AFM images of QD samples grown at 440 °C (top row), 470 °C (middle row), and 500 °C (bottom row), not annealed, annealed for 1, 5, and 10 min (columns left to right).

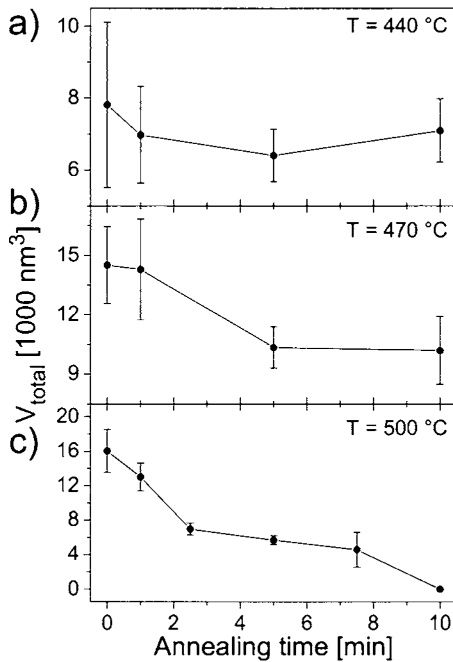

FIG. 6. Plot of total volume as a function of annealing time at (a) 440 °C, (b) 470 °C, and (c) 500 °C, respectively. The total volume was obtained by integrating volume histograms and normalized to an area of 1×1 μm^2.

the dot surface area and the corresponding surface tension, leading to the observed reduction in the film force, for which a mathematical model is given below in the Discussion section.

Annealing at 455 and 470 °C shows a similar decrease in the film force; however, the final values reached (1.35 N/m at 455 °C and 1.1 N/m at 470 °C, respectively) are below the value of the film force obtained at the critical thickness. A comparison between the film force curves obtained during annealing of the wetting layer and the quantum dot samples shows that both curves end with similar values and display the same slope at the end of annealing. This indicates that, although the film force curve measured on quantum dot films contains some contribution from changes of the wetting layer during annealing, the dots undergo similar morphological changes as compared to annealing at 440 °C, as shown in Fig. 5.

To check that the evolution of the film force curve can be explained by a simple superposition of the F_F of the wetting layer and the quantum dots and is not caused by a mass transfer between the wetting layer and the QDs, we extracted total volume of all dots from volume histograms of the AFM images. Plots of the total volume (normalized to an area of 1×1 μm^2) as a function of annealing time are shown in Fig. 6. The obtained values are smaller for all images than the nominally deposited volume which is a result of a too low resolution (1024×1024 pixel) in the AFM images and also a resulting too low resolution in the volume histograms, in which the perimeter of all dots as well as very small dots is not counted. However, due to this consistent error, only the absolute values in the total volume are shifted while the time dependence is not altered. For annealing at 440 °C as well as 470 °C, the total volume remains within the error bars constant, indicating standard Ostwald ripening behavior, thereby justifying the assumption that no interdiffusion takes place.

The film force curve of the QD sample annealed at 500 °C for 10 min reaches a value below the final value approached during annealing of the corresponding wetting-layer sample. One possibility could be the formation of dislocation in the QD film. However, high-resolution transmission electron microscopy has shown that no dislocations are formed. Another possibility could be a large mass transfer from the wetting layer to the dots and subsequent dot dissolution due to In desorption, as already observed at higher annealing temperatures.[12] The AFM images shown in the bottom row of Fig. 5 indeed reveal that the quantum dots dissolve and a plot of the total volume [Fig. 6(c)] clearly shows that the amount of material in the dots decreases during annealing. Therefore, in order to develop a model for the observed annealing behavior at high temperature, both mass transfer between substrate, wetting layer, and quantum dots via interdiffusion of Ga and In and In desorption from the QDs must be considered.

IV. DISCUSSION

A. Annealing at low temperatures

For annealing at low temperatures, we have observed standard ripening from small to large dots. The total volume of all dots remains constant as shown in Fig. 6, we therefore employ the following simplified model for the film force curves obtained at low annealing temperatures. As an approximation, we assume a constant surface tension σ for the dots with the total surface area of the dots A_{dots} changing with time. For such a situation, the film force $F_F(t)$ is given by

$$F_F(t) \propto \sigma[A_{\text{dots}}(t)/A_{\text{subs}}], \tag{2}$$

where A_{subs} is the constant surface area of the substrate. This can, however, also be extended to a more complicated form, for instance, by assuming different surface tension values for various dot facets. A close look at the AFM images presented in Fig. 5 reveals that the overall dot shape remains constant; therefore, such an extension would lead to constant geometry factor in the film force. We are, however, only interested in fitting normalized curves; therefore our simplified model is sufficient. Since the dots show three-dimensional coarsening, we start with a model developed by Vengrenovitch for ripening of three-dimensional particles.[10] According to this model, at a given time t, the maximum radius of the particles r_g is given by

$$r_{g_n}(t) = a_n(t + b_n)^{1/(n+1)} \quad \text{with } b_n = r_{0g}^{n+1}/a_n, \tag{3}$$

where r_{0_g} and a_n are constants, which depend on various material parameters and are therefore temperature dependent. For $n=1$, the ripening will be controlled by attachment or detachment of atoms on the dot surface, for $n=2$, the mechanism for QD ripening is limited by surface diffusion of atoms while for $n=3$ the ripening is limited by diffusion of atoms

along grain boundaries. Since the total volume of all dots remains constant during the ripening process, the distribution of particle sizes r at time t is then calculated as

$$f_n(r,t) = \text{const}_n \int_0^{r_{g_n}(t)} \frac{g_n(r/r_{g_n}(t))}{r_{g_n}(t)^4} dr, \tag{4}$$

with distribution functions

$$g_1(u) = u(1-u)^{-4} \exp(-2/(1-u)), \tag{5}$$

$$g_2(u) = u(1-u)^{-28/9}(u+2)^{-17/9} \exp[-2/(3(1-u))], \tag{6}$$

and

$$g_3(u) = \frac{u^3 \exp[-1/[3(1-u)]]\exp[-(1/9\sqrt{2})\arctan((u+1)/\sqrt{2})]}{(1-u)^{25/9}(u^2+2u+3)^{29/18}} \tag{7}$$

derived by Wagner,[9] Lifshitz and Slezov,[8] and Vengrenovitch.[10] The overall dot surface area $A_{\text{dots}_n}(t)$ then is

$$A_{\text{dots}_n}(t) \propto \pi \int_0^{r_{g_n}(t)} r^2 f_n(r,t) dr. \tag{8}$$

During calculation for each model a_n is normalized, which simplifies the analysis by removing additional temperature dependent factors. We choose different b_n to fit the experimental curves and get the value of b_n according to the minimum of relative errors.

Our calculation results are shown in Fig. 7. For annealing at 440 °C, model 3 yields the best fit to the experimental curve, i.e., ripening controlled by atom diffusion along dot boundar fits. However, the other two models also closely fit the experimental data. It is therefore difficult to clearly distinguish which mechanism really limits the ripening process of dots or if a combination of two or more mechanisms governs the process. On the other hand, for annealing at 455 and 470 °C, model 1 fits the experimental data very well, indicating that the kinetic process, in which attachment/detachment of atoms on the dot surface is the limiting step, is the mechanism for dot ripening. Considering that diffusion is typically a limiting factor at lower temperatures and kinetic processes are the limiting factors at higher temperatures, our results appear reasonable. It must be noted that the film force curves obtained at 455 and 470 °C also contain a contribution of changes in the wetting layer during annealing; however, these changes are relatively small and are not dominant at the beginning of annealing where the largest change in film force is due to the ripening of the dots. We also fitted curves for which the contribution of the wetting layer was subtracted and obtained again the same models. This can be explained by the fact that the fits are more sensitive to the beginning part of the film force curves and therefore fitting of the original data sets is still valid. Due to the employed fitting of the experimental data with a model which incorporates the whole time evolution of the dot distribution function rather than only an average dot radius, our results are more compelling in determining the ripening process compared to previously published work.

B. Annealing at high temperatures

Since the quantum dots dissolve during annealing at 500 °C, the assumption that the volume remains constant is no longer valid, as can be clearly seen in a plot of the total volume of all dots shown in Fig. 6. We can therefore not use the above model. However, we can explain our observations in the following way. Let us consider the whole system composed of quantum dots, wetting layer, and substrate as a supersaturated solution of In in a GaAs matrix. For such a system, a critical radius R_{cr} exists for each quantum dot and depends on the degree of supersaturation Δ, which is proportional to the In concentration. The critical radius is given by α/Δ, where α is a constant associated with the surface tension of the dots. When the dot radius is larger than the critical radius, the dot grows, otherwise it dissolves. At elevated

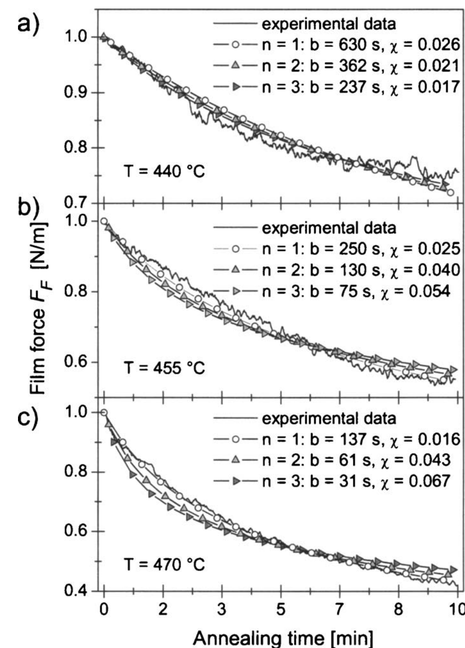

FIG. 7. Fits to film force curves measured as a function of annealing time at (a) 440 °C, (b) 455 °C, and (c) 470 °C.

temperatures,[14] one has to consider both In desorption and interdiffusion between In in the dots and the wetting layer and Ga from the substrate. At the beginning stage of annealing, the In concentration in dots is high, leading to a small critical radius. Those dots with a larger radius r grow at the expense of those dots with a smaller radius r and standard ripening is still observed. With further annealing, due to In desorption and In/Ga interdiffusion, the In concentration decreases and the critical radius increases, leading to fewer and fewer dot ripening. Eventually, the increase in R_{cr} overtakes the increase of the mean dot radius r_{mean}, i.e.,

$$dR_{cr}/dt > dr_{mean}/dt, \tag{9}$$

leading to a shrinking and eventual dissolution of more and more dots. After a certain time, R_{cr} is larger than the largest dot radius r_{max} resulting in a dissolution of all dots. This process is clearly seen in our AFM images taken at later annealing stages.

V. CONCLUSIONS

We have studied the ripening of InAs quantum dots grown on GaAs(001) substrates by *in situ* measuring the stress during growth and subsequent annealing. For annealing at low temperatures, a model based on Ostwald ripening was developed that allows us to fit the relaxation curves and determine which mechanism plays the main role. We find that, for annealing InAs/GaAs(001) at 440 °C, it is difficult to determine the ripening process exactly, but still a model describing ripening controlled by atom diffusion along dot boundaries fits the experimental data best. On the other hand, for annealing at 455 and 470 °C, we find that the ripening process is clearly limited by atom attachment/detachment on the dot surface. For annealing at 500 °C, the different evolution process can be explained by a combination of interdiffusion between Ga and In atoms and desorption of In.

ACKNOWLEDGMENTS

The authors thank S. Krauß for experimental help, Dr. A. Trampert for assistance with HRTEM, and Dr. V. Kaganer for useful discussions. This work was supported by the Deutsche Forschungsgemeinschaft (SFB 296).

[1] See, e.g., M. Grundmann, Physica E (Amsterdam) **5**, 167 (2000), and references therein.
[2] I. N. Stranski and L. Krastanow, Sitzungsber. Akad. Wiss. Wien, Math.-Naturwiss. Kl., Abt. 2B **146**, 797 (1937).
[3] D. M. Schaadt, S. Krauss, R. Koch, and K. H. Ploog, Appl. Phys. A: Mater. Sci. Process. (to be published).
[4] M. Moison, F. Houzay, F. Barthe, L. Leeprince, E. Andre, and O. Vatel, Appl. Phys. Lett. **64**, 196 (1994); J. Y. Marzin, J. M. Gerard, A. Izrael, D. Barrier, and G. Bastard, Phys. Rev. Lett. **73**, 716 (1994).
[5] W. Ostwald, Z. Phys. Chem. (Leipzig) **34**, 495 (1990).
[6] K. Poetschke, L. Mueller-Kirsch, R. Heitz, R. L. Sellin, U. W. Pohl, D. Bimberg, N. Zakharov, and P. Werner, Physica E (Amsterdam) **21**, 606 (2004).
[7] T. J. Krzyzewski and T. S. Jones, J. Appl. Phys. **96**, 668 (2004).
[8] I. M. Lifshitz and V. V. Slezov, Sov. Phys. JETP **35**, 331 (1959); J. Phys. Chem. Solids **19**, 35 (1959).
[9] C. Wagner, Z. Elektrochem. **65**, 581 (1961).
[10] R. D. Vengrenovitch, Acta Metall. **30**, 1079 (1982).
[11] R. D. Vengrenovitch, Yu. V. Gudyma, and S. V. Yarema, Semiconductors **35**, 1378 (2001).
[12] Ch. Heyn, Phys. Rev. B **66**, 075307 (2002).
[13] H. Lee, R. R. Lowe-Webb, W. Yang, and P. C. Sercel, Appl. Phys. Lett. **71**, 2325 (1997).
[14] P. B. Joyce, T. J. Krzyzewski, G. R. Bell, B. A. Joyce, and T. S. Jones, Phys. Rev. B **58**, R15981 (1998).
[15] B. A. Joyce, T. S. Jones, and J. G. Berk, J. Vac. Sci. Technol. B **16**, 2373 (2005).
[16] B. Lita, R. S. Goldman, J. D. Phillips, and P. K. Bhattacharya, Surf. Rev. Lett. **7**, 539 (2000).
[17] R. Koch, G. Wedler, J. J. Schulz, and B. Wassermann, Phys. Rev. Lett. **87**, 136104 (2001).
[18] G. G. Stoney, Proc. R. Soc. London, Ser. A **32**, 172 (1909).
[19] R. P. Mirin, A. Roshko, and M. van der Puijl, J. Vac. Sci. Technol. B **20**, 1489 (2002).
[20] D. J. Bottomley, Appl. Phys. Lett. **72**, 783 (1998).